PHILOSOPHICAL TRANSACTIONS A

royalsocietypublishing.org/journal/rsta

Research

Cite this article: Amaral PHR, Stanke M, Adamowicz L, Diniz LG, Mohallem JR, Alijah A. 2019 Non-adiabatic effects in the H_3^+ spectrum. *Phil. Trans. R. Soc. A* **377**: 20180411. http://dx.doi.org/10.1098/rsta.2018.0411

Accepted: 3 April 2019

One contribution of 18 to a discussion meeting issue 'Advances in hydrogen molecular ions: H_3^+, H_5^+ and beyond'.

Subject Areas:
spectroscopy, chemical physics, atomic and molecular physics, chemical physics

Keywords:
theoretical high-resolution spectroscopy, rovibrational states, non-adiabatic effect, effective reduced mass

Author for correspondence:
Alexander Alijah
e-mail: alexander.alijah@univ-reims.fr

Non-adiabatic effects in the H_3^+ spectrum

Paulo H. R. Amaral[1], Monika Stanke[2], Ludwik Adamowicz[3], Leonardo G. Diniz[4], José R. Mohallem[1] and Alexander Alijah[5]

[1]Department of Physics, Federal University of Minas Gerais, PO Box 702, 30123-970 Belo Horizonte, Minas Gerais, Brazil
[2]Institute of Physics, Faculty of Physics, Astronomy and Informatics, Nicolaus Copernicus University, ul. Grudziądzka 5, Toruń 87-100, Poland
[3]Department of Chemistry and Biochemistry, The University of Arizona, Tucson, AZ 85721, USA
[4]CEFET Minas Gerais, 30421-169 Belo Horizonte, Minas Gerais, Brazil
[5]Groupe de Spectrométrie Moléculaire et Atmosphérique, UMR CNRS 7331, University of Reims Champagne-Ardenne, 51687 Reims Cedex 2, France

AA, 0000-0002-4915-0558

The effect of non-adiabatic coupling on the computed rovibrational energy levels amounts to about $2\,cm^{-1}$ for H_3^+ and must be included in high-accuracy calculations. Different strategies to obtain the corresponding energy shifts are reviewed in the article. A promising way is to introduce effective vibrational reduced masses that depend on the nuclear configuration. A new empirical method that uses the stockholder atoms-in-molecules approach to this effect is presented and applied to H_3^+. Furthermore, a highly accurate potential energy surface for the D_3^+ isotopologue, which includes relativistic and leading quantum electrodynamic terms, is constructed and used to analyse the observed rovibrational frequencies for this molecule. Accurate band origins are obtained that improve existing data.

This article is part of a discussion meeting issue 'Advances in hydrogen molecular ions: H_3^+, H_5^+ and beyond'.

Electronic supplementary material is available online at https://doi.org/10.6084/m9.figshare.c.4545917.

THE ROYAL SOCIETY PUBLISHING

1. Introduction

Rovibrational molecular states are routinely computed within the Born–Oppenheimer approximation using standard quantum chemical electronic structure methods and standard basis sets. The precision that can be obtained with such a procedure is far from reaching that of spectroscopic measurements. The first problem is related to the use of standard Gaussian basis sets that, even when extrapolated to the so-called complete basis set limit, are not satisfactory as they do not satisfy the boundary conditions of the electronic Schrödinger equation at both short and large distances. The introduction of electronic basis functions that depend explicitly on inter-particle (inter-electron) distances, even if they still have Gaussian forms, allows one to better satisfy the cusp conditions [1,2] as two particles approach each other, and greatly improves the Born–Oppenheimer electronic energy. One of the first potential energy surfaces of this type was published in 1998 by Cencek *et al.* [3]. Adding the energy of the diagonal adiabatic correction to the Born–Oppenheimer energy yielded an adiabatic surface accurate to about 0.1 microhartree or $0.02\,\mathrm{cm}^{-1}$. The effect of the diagonal adiabatic correction on the vibrational energies is of the order of 1–$2\,\mathrm{cm}^{-1}$ for H_3^+, relative to the vibrational zero-point energy. The adiabatic correction term is significant for light molecules, as it scales as one over the nuclear mass. With a very accurate adiabatic potential energy surface at hand, it is appropriate to include relativistic [3] and even quantum electrodynamic (QED) contributions [4], which both affect the vibrational energies by about $0.2\,\mathrm{cm}^{-1}$. Very accurate potential energy surfaces have been published within recent years [3,5–7]; for a review, see Tennyson *et al.* [8]. Adamowicz, Stanke and co-workers recently developed algorithms for calculating the leading relativistic and QED terms with improved precision for a molecule with an arbitrary number of electrons [9], and these algorithms have been used in the present work, together with the adiabatic energy values published earlier [6]. However, non-adiabatic coupling, which is due to the off-diagonal terms of the nuclear kinetic energy operator in the basis of the adiabatic electronic wave functions, affects the computed vibrational energy levels by the same order of magnitude as the diagonal correction term. Hence this effect needs to be accounted for in high-accuracy computations. Unlike the other above-mentioned effects, due to its dynamical nature, the non-adiabatic effect cannot be described as a correction to the Born–Oppenheimer potential energy surface.

For the diatomic H_2, with two electrons just as H_3^+, impressive accuracy has been achieved, starting from the seminal work of Kołos & Wolniewicz [10], and culminating in the latest achievements by Pachucki, Komasa and co-workers [11–14] and by Nakatsuji and co-workers [15, 16]. In these works, non-adiabatic, relativistic and QED corrections were computed from first principles.

The procedures used to calculate the non-adiabatic effects in the above-cited works are highly specialized and cannot be easily transferred to the triatomic H_3^+. Empirical approaches have instead been developed and will be reviewed in this article. Obviously, empirical approaches cannot compete with the sophisticated *ab initio* approaches used for H_2, and cannot be expected to recover 100% of the non-adiabatic energy shifts for H_2 and H_2^+. However, they are straightforward to use and yield physical insight. Due to the developments by Adamowicz and co-workers, we now have electronic energies calculated with outstanding accuracy for several systems, including H_3^+, at our disposal. If these can be represented and interpolated with the same accuracy, any deviation between computed and experimentally derived rovibrational energies can be attributed to non-adiabatic effects, thus providing a testbed for the development of non-adiabatic models.

2. Effective mass approaches

In principle, the effect of non-adiabatic coupling on rovibrational states can be evaluated by integration of the system of coupled equations for the nuclear motion resulting from the adiabatic ansatz, in which the total wave function is expanded in a basis of electronic eigenfunctions. If the electronic state of interest is sufficiently decoupled from other electronic states, the multi-state problem may be reduced to an effective one-state problem, as has first been shown for diatomic

molecules by Herman & Asgharian [17] using perturbation theory and by Bunker & Moss [18] using contact transformations. Their formulations lead to effective Hamiltonians, in which the vibrational and rotational reduced masses are not only different but have now also become functions depending on the nuclear coordinates. Furthermore, there is an additional correction term to the potential, W_{NA}, which enters the nuclear-motion equation:

$$H = -\frac{\nabla_R^2}{2\mu_{\mathrm{vib}}(R)} + \frac{J(J+1)}{2\mu_{\mathrm{rot}}(R)R^2} + W(R) \tag{2.1}$$

and

$$W(R) = W_0(R) + W_{\mathrm{A}}(R) + W_{\mathrm{NA}}(R). \tag{2.2}$$

The other quantities in the above equations are R, the internuclear distance, J, the angular momentum quantum number, $W_0(R)$, the Born–Oppenheimer energy curve, and $W_{\mathrm{A}}(R)$, the diagonal adiabatic correction; $\mu_{\mathrm{vib}}(R)$ and $\mu_{\mathrm{rot}}(R)$ are the R-dependent vibrational and rotational reduced masses, respectively. Atomic units have been used.

Different approaches to determine vibrational reduced masses have been proposed by Kutzelnigg [19], Jaquet & Kutzelnigg [20] and Mátyus [21,22], all applicable to diatomic molecules. Bunker & Moss [18] extended the formalism to triatomic molecules [23], and it was applied to the water molecule by Schwenke [24]. Khoma & Jaquet [25], starting from the work of Herman & Asgharian [17], derived an effective rovibrational Hamiltonian for H_3^+ and computed vibrational [26] and rovibrational [27] states for this molecule. Their results demonstrated, as did the application of the Bunker & Moss [18] theory to the LiH molecule by Tyuterev and co-workers [28], that, despite considerable computational and numerical difficulties, the numerical results were not yet satisfactory. More practical, empirical approaches to the rovibrational problem have also been developed. Moss [29] derived a constant vibrational mass for the H_2^+ molecule, which is $m_{\mathrm{Moss}} = m_{\mathrm{p}} + 0.47531 m_{\mathrm{e}}$, where m_{p} and m_{e} denote the proton and electron masses, respectively. In his approach, the rotational mass was left equal to the nuclear mass. Mass m_{Moss}, which has become known as Moss mass, was then introduced to the theoretical spectroscopy of H_3^+ by Polyansky & Tennyson [30]. It worked extraordinarily well, but, as has been demonstrated later, the excellent performance was fortuitous and partially due to error cancellation [4]. These authors computed vibrational states using the very accurate adiabatic GLH3P potential energy surface [6], to which relativistic corrections were added. Unfortunately, inclusion of QED effects made the agreement with the experimental data slightly worse, as can be seen from table VI of Lodi *et al.* [4].

(a) Vibrational and rotational shifts by scaling

The non-adiabatic vibrational shifts are one order of magnitude stronger than the non-adiabatic rotational shifts. The reason is that the vibrating nuclei change their direction of motion at the classical turning points and the electrons lag behind. This interpretation of the non-adiabatic effects has led to an empirical formula for the vibrational shifts that incorporates the derivative of the potential with respect to the nuclear displacement from equilibrium [31,32]. The method reproduces approximately 90% of the non-adiabatic shift in the case of H_2 and its isotopologues, which for these molecules amounts to about $5\,\mathrm{cm}^{-1}$. The approach has never been tested for H_3^+.

In their earlier work on H_3^+, Alijah and co-workers applied the empirical shifts obtained as differences between computed and experimental data to the band origins, first to the deuterated isotopologues, H_2D^+, D_2H^+ and D_3^+ [33–35], and later to H_3^+ [36]. For the latter system, the shifts determined for states below the barrier to linearity ($\approx 10\,000\,\mathrm{cm}^{-1}$) can be expressed as

$$\Delta E = E_{\mathrm{obs}} - E_{\mathrm{calc}} = a_0 + a_1 J(J+1) + a_2 G^2, \tag{2.3}$$

where $G = |k - \ell|$ is Watson's [37] quantum number, with k the a-axis projection of J and ℓ the vibrational angular momentum quantum number associated with the degenerate vibration v_2: $\ell = -v_2, -v_2 + 2, \ldots, +v_2$. The constants a_0, a_1 and a_2 are characteristic and specific to each vibrational

band. They can be parametrized in an efficient way. The vibrational shift parameter, a_0, is a linear function of the energy and can be approximated as $a_0 = b_1 E^0_{\mathrm{calc}}$, where E^0_{calc} denotes the calculated energy of the band origin. For the rotational parameters, unique average values derived from all rotational transitions can be used. In this way, the following empirical formula was obtained:[1]

$$E_{\mathrm{exact}} \approx E_{\mathrm{calc}} + \Delta E = E_{\mathrm{calc}} + b_1 E^0_{\mathrm{calc}} + \bar{a}_1 J(J+1) + \bar{a}_2 G^2. \tag{2.4}$$

The numerical values of the parameters are $b_1 = -1.0123(41) \times 10^{-4}\,\mathrm{cm}^{-1}$, $\bar{a}_1 = -2.0436 \times 10^{-3}\,\mathrm{cm}^{-1}$ and $\bar{a}_2 = -1.3600 \times 10^{-3}\,\mathrm{cm}^{-1}$. In the case where spectroscopic quantum numbers have not been assigned to a computed rovibrational state, the energy, E_{calc}, may be scaled directly with the b_1 parameter, however, with some loss of accuracy. With that, extrapolation has become possible and has allowed predicting frequencies at higher energy range (up to $12\,000\,\mathrm{cm}^{-1}$) for states not yet observed [38]. This was extended to the energy region of up to $15\,300\,\mathrm{cm}^{-1}$ [39] after replacing the simple linear b_1 scaling with a quadratic scaling, for which numerical values of the scaling parameters were obtained with the help of the new experimental data [40,41]. The predictions made in the above-mentioned papers were useful to guiding the measurements performed by Wolf and co-workers [42] at the Max Planck Institute in Heidelberg. Extremely weak vibrational overtone lines were measured using an action spectroscopy method. The strongest lines were identified with the help of the line list provided by Neale *et al.* [43]. The line positions from that work provided an upper bound for the frequency scan, while those from [38] provided a lower bound [44]. New computations performed with the use of the GLH3P potential energy surface and the Moss vibrational masses gave close agreement with the experimental frequencies [44]. The smallness of the rotational parameters, $\bar{a}_1$ and $\bar{a}_2$, demonstrated that the rotational non-adiabatic correction is one order of magnitude smaller than the vibrational correction. Furthermore, due to the fact that the rotational transitions obey the angular momentum selection rule $\Delta J = 0, \pm 1$, and hence the absolute J-dependent errors are similar for the two states, these errors almost cancel out when energy differences are formed. Therefore, the computed rotational transition frequencies are more accurate than the term values themselves (10^{-3}–$10^{-2}\,\mathrm{cm}^{-1}$ for moderate values of J).

(b) Vibrational and rotational shifts by effective mass models

In a paper published in 2007, Kutzelnigg [19] addressed the question of 'Which masses are vibrating or rotating in a molecule?' and analysed the cases of H_2 and H_2^+. Explicit formulae for effective masses for these molecules were derived starting from an LCAO (linear combination of atomic orbitals) approach. This inspired Mohallem and co-workers [45] to formulate a theory of separation of motions of core and valence electrons. In their approach, the electronic density is divided into a core density that closely follows the nuclei as they vibrate, and a valence density that participates in the formation of the chemical bond and moves less with the vibrations. The mass of the core fraction is then added to the nuclear mass, m_{A}, to yield

$$m_{\mathrm{A}}(R) = m_{\mathrm{A}} + n_{\mathrm{AA}}(R) m_{\mathrm{e}}. \tag{2.5}$$

Different empirical approaches have then been tested to obtain the core fraction of the electronic density, n_{AA}. The first idea was to obtain this fraction from the Mulliken population analysis; more precisely, from the diagonal elements of the population matrix. In the work by Diniz *et al.* [46], this approach was applied to H_2^+, H_2 and their isotopologues. Using the atomic core masses of equation (2.5), the reduced vibrational mass of molecule AB was then obtained in the usual way as

$$\frac{1}{\mu_{\mathrm{vib}}(R)} = \frac{1}{m_{\mathrm{A}}(R)} + \frac{1}{m_{\mathrm{B}}(R)}. \tag{2.6}$$

In the work of Diniz *et al.* [46], the electronic structure calculations to determine the Mulliken populations were performed at the CI/cc-pV5Z level of theory. The non-adiabatic shifts of the

[1]In [36], ΔE was defined as $\Delta E = E_{\mathrm{calc}} - E_{\mathrm{obs}}$. The numerical values of the parameters are thus the negative of those given in the present review.

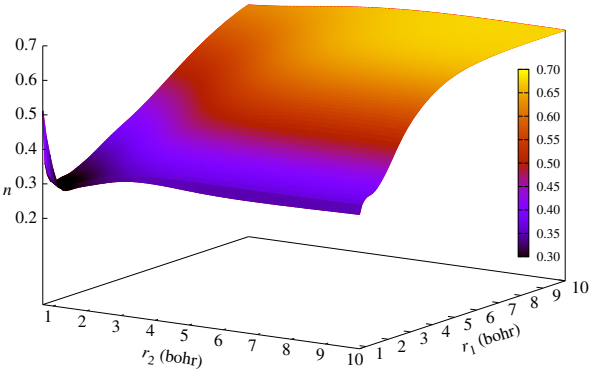

Figure 1. Visualization of the vibrational mass surface for configurations with the C_{2v} symmetry. r_1 is the atom–diatom distance and r_2 the diatomic distance. Reproduced with permission from [50].

vibrational energies were then determined as a difference between the results obtained using the effective reduced mass defined above and the results obtained using the nuclear reduced mass. Very good agreement was found when the calculated shifts were compared with the exact values of Wolniewicz & Poll [47] for H_2^+ and of Wolniewicz [48,49] for H_2. Moreover, after application of a scaling factor, the agreement with the exact data was almost perfect. The agreement was also very good for the mixed isotopologues, for which the non-adiabatic calculations using the traditional approach are more complicated due to symmetry breaking. The need to use a scaling factor is perhaps not surprising. It is well known that the electronic density does not always converge to a single limit as the basis set is increased, in contrast to the energy, whose convergence is governed by the variational principle.

The above method has then been also applied to H_3^+ [50]. Note that, in general, the form of the reduced mass depends on the coordinate system used. It can make sophisticated non-empirical approaches for determining the vibrational mass very cumbersome. In our method, no particular difficulty arises, as the reduced masses are obtained using the standard formulae, in which the nuclear masses are simply replaced by the nuclear core masses. As the nuclear core masses are configuration-dependent, so are the reduced masses. In the work of Diniz *et al.* [50], the first ever vibrational mass surface for a triatomic molecule was obtained. That surface is shown in figure 1. It is expressed in terms of Jacobi coordinates. At equilibrium, when all three bond lengths are $1.65a_0$, the electronic contribution to the core mass is about $0.3m_e$. If effective masses are to be used in rovibrational calculations, the algorithm used in the calculations needs to allow for the use of masses that are dependent on the nuclear geometry of the molecule. Such algorithms (and the corresponding computer programs) exist for diatomic [51] and for triatomic [52] molecules. Alternatively, the rovibrational problem may be solved iteratively, starting from the nuclear mass, as

$$\bar{m}_{A,v}^{(i+1)} = m_A + m_e \int \bar{n}(\boldsymbol{R}) \left[\chi_v^{(i)}(\boldsymbol{R})\right]^2 \mathrm{d}\boldsymbol{R}, \tag{2.7}$$

where $\chi_v^{(i)}(\boldsymbol{R})$ is the vibrational wave function obtained with the mass $\bar{m}_{A,v}^{(i)}$, and $\bar{n}(\boldsymbol{R})$ denotes the mass surface; v stands for the set of vibrational quantum numbers, which for H_3^+ are v_1, v_2, ℓ. In our work, we used the DVR3D computer program [53]. A satisfactory convergence is typically achieved after one iteration step. Note that such an iterative approach leads to a different constant reduced vibrational mass for each vibrational state, v.

DVR3D does not use the full permutational symmetry of the nuclei. Thus, for H_3^+ with three identical nuclei the two components of the degenerate representations are obtained in two independent calculations. Their energies should be the same within the numerical accuracy used in the calculation. This was also numerically verified when the core masses were employed in

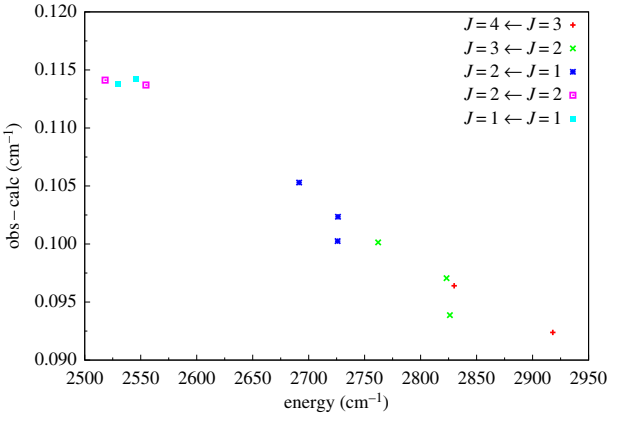

Figure 2. Obs – calc frequency differences obtained with the Moss mass model.

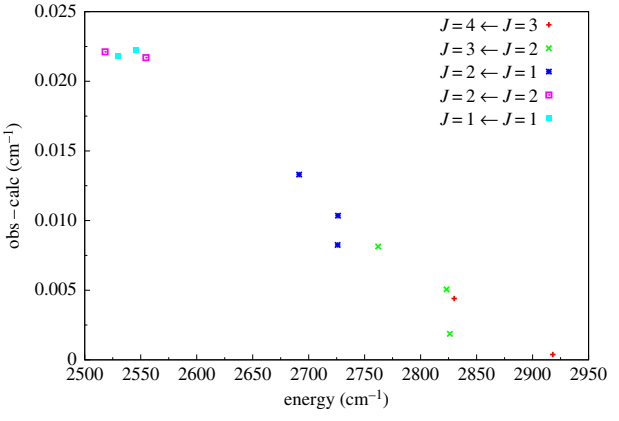

Figure 3. Obs – calc frequency differences obtained with the core mass model.

the calculation, even though the two vibrational masses were not identical. Conservation of the degeneracy validates our empirical ansatz.

The core mass approach was tested by comparing the calculated transition frequencies of 12 lines of the ν_2 band with the experimental frequencies that were measured with the outstanding accuracy of $\approx 10^4\,\mathrm{cm}^{-1}$ by Wu *et al.* [54]. Figures 2 and 3 show the performance of the Moss mass model by Polyansky & Tennyson [30] and the core mass model. Nuclear masses were used as the rotational masses in both cases. Vibrational offsets can be identified from the four R-branch ($\Delta J = 0$) transitions, which are about $0.1\,\mathrm{cm}^{-1}$ in the case of Moss masses and are reduced by a factor of five in the case of core masses, without any additional scaling. There clearly is a J-dependent rotational shift that is linear in J. This shift is consistent with the correction term in equation (2.4). This deviation was modelled using the empirical rotational mass correction surface suggested by Diniz *et al.* [46]. Additionally, when a scaling factor was applied to the vibrational mass, an excellent agreement was observed, as shown in figure 4. The approach has also been proven applicable to D_3^+ in Diniz *et al.*'s work, using identical parameter values. The experimental paper by Wu *et al.* [54] and our theory paper [50] were published back-to-back.

It should be mentioned that Mátyus and co-workers [52] extended the original GENIUSH rovibrational code [55] to incorporate coordinate-dependent vibrational masses and used it to optimize the vibrational mass in order to reproduce the 12 experimental lines. Their vibrational mass is practically identical to our core mass before scaling.

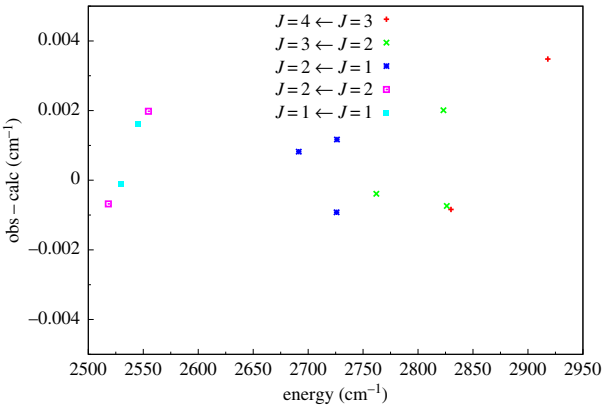

Figure 4. Obs – calc frequency differences obtained with a model employing scaled core masses and empirical rotational masses.

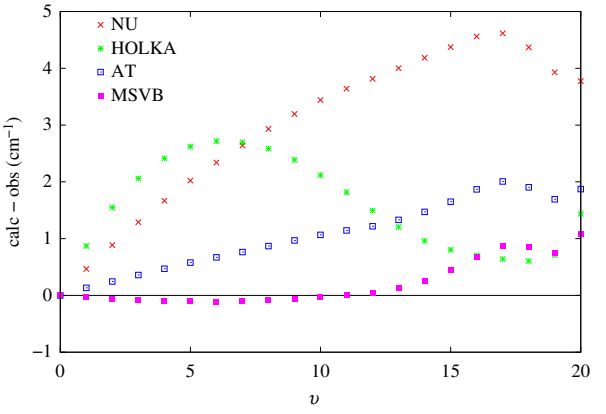

Figure 5. Calc – obs frequency differences for ^{7}LiH. NU, nuclear masses; HOLKA, [28]; AT, atomic masses; MSVB, multi-structure valence-bond masses, equation (2.8). The experimental data are from Coxon & Dickinson [57].

Diniz *et al.*'s [46] strategy to extract the core fraction of the electronic density using the Mulliken population analysis has been proven to be highly successful in describing the non-adiabatic shifts for the molecules comprising only hydrogen. These are non-polar molecules. A question has thus arisen whether the method performs equally well for polar molecules. An ideal test molecule is lithium hydride, LiH. It has an ionic structure at equilibrium, but becomes covalent at larger distances and dissociates into two neutral atoms. This behaviour has been explained by Mulliken [56] and is due to an avoided crossing of the two lowest singlet adiabatic potential energy curves. The method of Diniz *et al.* [46] yields results equivalent to those obtained using the atomic masses in calculating the reduced vibrational mass. Figure 5 shows that such a mass is not sufficiently large to reach satisfactory agreement with the experimental results. Disappointingly, the sophisticated method by Holka *et al.* [28] that uses the Bunker & Moss [18] procedure, performs worse than the simple ad hoc method that uses the atomic masses. Considering the ionic–covalent nature of LiH, Diniz *et al.* [58,59] devised a different approach in which they described the electronic wave function of LiH as a superposition of an ionic and a covalent configuration. The distance-dependent weights of the two configurations in the wave function were then used to superimpose the two corresponding reduced masses:

$$\mu_{\mathrm{vib}}(R) = c_{\mathrm{ionic}}(R)\frac{m_{\mathrm{Li}^+}m_{\mathrm{H}^-}}{m_{\mathrm{Li}^+}+m_{\mathrm{H}^-}} + c_{\mathrm{covalent}}(R)\frac{m_{\mathrm{Li}}m_{\mathrm{H}}}{m_{\mathrm{Li}}+m_{\mathrm{H}}}. \tag{2.8}$$

The ionic reduced mass is larger than the covalent reduced mass. For the ^{7}LiH isotopologue, for example, the nuclear, covalent (atomic) and ionic reduced masses are $1605.58701112m_e$, $1606.39892550m_e$ and $1607.14764909m_e$, respectively. Then $\mu_{vib}(R)$ is also larger than the atomic reduced mass, for any non-zero ionic contribution, which we interpret as due to participation of excited electronic states in the nuclear motion. It yields the best vibrational energies obtained so far for the LiH molecule (figure 5). For $v = 13$, the deviation between the experimental and theoretical data increases, as the probability of the average internuclear distance getting closer to the distance where the avoided crossing between the two lowest electronic states occurs, increases. Extended line lists and tables of cooling functions were compiled for LiH comprising lithium isotopes ^{6}Li and ^{7}Li and hydrogen isotopes H, D and T [60].

(c) Vibrational shifts by effective mass models: a unifying AIM approach

Though the results obtained so far are encouraging, the fact that two different methods should be used, depending on whether the molecule is polar or non-polar (e.g. in the LiH calculations), is not satisfactory. Amaral & Mohallem [61] recently developed a unifying single method which uses the stockholder atoms-in-molecules (AIM) approach by Hirshfeld [62], more precisely its iterative variant, Hirshfeld-I due to Bultinck *et al.* [63], to separate the core and valence electron density contributions. In his approach, Hirshfeld defined the density of a 'promolecule', which is the sum of the densities of the isolated atoms, as

$$\rho^{\mathrm{pro}}(\mathbf{r}) = \sum_I \rho_I^{\mathrm{at}}(\mathbf{r}). \tag{2.9}$$

He then introduced the following atomic weight functions:

$$w_I(\mathbf{r}) = \frac{\rho_I^{\mathrm{at}}(\mathbf{r})}{\rho^{\mathrm{pro}}(\mathbf{r})}, \tag{2.10}$$

which, when applied to the molecular density, give the AIM densities. For atom I, this density is

$$\rho_I^{\mathrm{AIM}}(\mathbf{r}) = w_I(\mathbf{r})\rho^{\mathrm{mol}}(\mathbf{r}). \tag{2.11}$$

Within the iterative Hirshfeld-I scheme, the weight function and promolecule atomic densities are updated such as to make the atomic populations in the promolecule identical to those of the atoms in molecules. Amaral & Mohallem [61] defined an atomic potential within the molecule as

$$V_I(\mathbf{R}, \mathbf{r}) = -\int_{|\mathbf{r}'-\mathbf{R}_I|=0}^{\mathbf{r}} \frac{Z_I - \rho^{\mathrm{mol}}(\mathbf{r}', \mathbf{R})}{|\mathbf{r}' - \mathbf{R}_I|}\, \mathrm{d}\mathbf{r}', \tag{2.12}$$

where the dependence of ρ and of V_I on the nuclear coordinates, $\mathbf{R}$, is indicated for the sake of clarity. The atomic potentials are used to divide the AIM electronic density into a core fraction and a valence fraction, depending on whether, at a nuclear configuration $\mathbf{R} = \mathbf{R}'$, the potential of atom A, $V_A(\mathbf{R}', \mathbf{r})$, is more attractive than the sum of the potentials of the other atoms, V_B, V_C, etc., or not:

$$V_A(\mathbf{R}', \mathbf{r}) \begin{cases} < V_B(\mathbf{R}', \mathbf{r}) + V_C(\mathbf{R}', \mathbf{r}) + \cdots, & \mathbf{r} \in \text{ core region}, \\ = V_B(\mathbf{R}', \mathbf{r}) + V_C(\mathbf{R}', \mathbf{r}) + \cdots, & \mathbf{r} \text{ on division line}, \\ > V_B(\mathbf{R}', \mathbf{r}) + V_C(\mathbf{R}', \mathbf{r}) + \cdots, & \mathbf{r} \in \text{ valence region}. \end{cases} \tag{2.13}$$

Integrating the AIM electronic density over the core region and adding the result to the nuclear mass,

$$m_A(\mathbf{R}) = m_A^{\mathrm{nuc}} + m_e \int_{\text{core region}} \rho_A^{\mathrm{AIM}}(\mathbf{r}, R)\, \mathrm{d}\mathbf{r}, \tag{2.14}$$

yields the effective AIM mass. This is illustrated in figure 6.

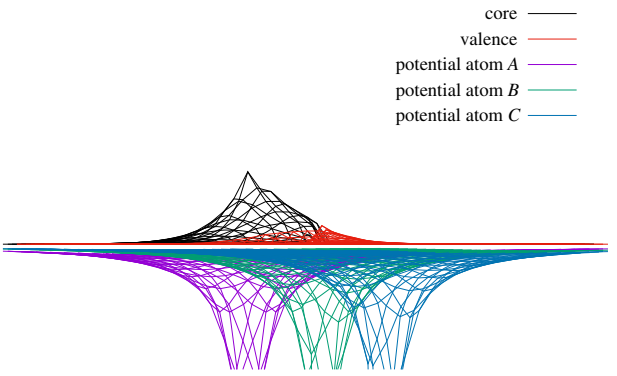

Figure 6. Determination of core and valence fractions within the AIM model, shown here for atom *A*.

(d) Vibrational shifts by *ab initio* effective masses

Jaquet & Khoma developed a procedure for determining effective masses from first principles [64] following the perturbative approach of Herman & Asgharian [17]. They also derived the kinetic energy operator for a triatomic molecule taking into account coordinate-dependent masses [26] and included the resulting correction terms in their rovibrational computer program [65]. Their H_3^+ mass surface contains contributions from as many as 499 excited singlet states. Rovibrational energies obtained in the calculations that used their approach were recently reported [25,27].

3. Results for H_3^+

In the present work, we have applied the stockholder AIM approach to H_3^+. The stockholder AIM mass was computed for all configurations of the DVR grid that was later used to calculate the energies of vibrational states with the DVR3D computer code. This ensures that the numerical integration involved in the iterative determination of the state-dependent vibrational reduced masses (see equation (2.7)) can be performed without loss of accuracy. We have then computed the band origins for which experimentally derived data are available from the MARVEL analysis [66] of 26 experimental sources. The GLH3P potential energy surface was employed. It was augmented with relativistic and QED corrections as described by Lodi *et al.* [4]. The results are presented in table 1, where they are contrasted with those obtained for the same surface with the non-adiabatic Moss mass model of Polyansky & Tennyson [30], the effective mass model of Diniz *et al.* [50] and the effective mass of Jaquet & Khoma [26]. The stockholder AIM results are clearly the most accurate. This is quite amazing considering the simplicity of the approach. Furthermore, both the Polyansky & Tennyson results and the Jaquet & Khoma results deteriorated when the QED correction was included, while the results of Diniz *et al.* and the present ones obtained with the AIM mass were improved.

4. Results for D_3^+

Adamowic, Stanke and co-workers [9] have recently implemented a new method to determine relativistic and leading QED (including the Araki–Shuchar term) corrections for wave functions expanded in terms of explicitly correlated Gaussians. With this, they have computed these terms for the same large grid defined in terms of hyperspherical coordinates as the one used by Pavanello *et al.* [6] for the calculation of the Born–Oppenheimer energies and the diagonal adiabatic corrections. The total energy that includes the Born–Oppenheimer, relativistic, QED and

Table 1. Computed band origins and differences exp – calc, in cm^{-1}. Nuc, nuclear mass; PT, Polyansky–Tennyson mass [30]; Din, Diniz mass [50]; this work, Stockholder AIM mass; JK, Jaquet–Khoma mass [26]. QED shifts were added to the JK values using the nuc data from [4].

(v_1, v_2^ℓ)	exp	this work (nuc)	PT	Din	JK	this work (AIM)
$(0, 1^1)$	2521.41	−0.14	0.16	0.05	0.10	0.11
$(0, 2^2)$	4998.04	−0.33	0.23	0.05	0.19	0.14
$(1, 1^1)$	5554.06	−0.71	−0.07	−0.28	−0.19	−0.16
$(0, 3^3)$	7492.91	−0.61	0.26	−0.03	0.35	0.12
$(2, 2^2)$	10645.38	−0.95	0.20	−0.16	0.08	0.05
$(0, 5^1)$	10862.90	−0.66	0.34	0.00	0.31	0.16
$(3, 1^1)$	11323.10	−1.14	0.11	−0.29	−0.08	−0.04
$(0, 5^5)$	11658.40	−0.90	0.27	−0.10	0.32	0.08
$(2, 3^1)$	12303.37	−0.95	0.22	−0.16	0.25	0.03
$(0, 6^2)$	12477.38	−0.98	0.18	−0.19	0.19	−0.01
$(0, 7^1)$	13702.38	−1.12	0.00	−0.41	0.02	−0.21
$(0, 8^2)$	15122.80	−1.06	0.38	−0.18	0.47	0.13
RMS		0.85	0.23	0.20	0.25	0.12

adiabatic energies is

$$E_{\mathrm{tot}}(\mathbf{R}) = E_{\mathrm{BO}}(\mathbf{R}) + E_{\mathrm{rel}}(\mathbf{R}) + E_{\mathrm{QED}}(\mathbf{R}) - \sum_{I=1}^{3} \frac{\langle \nabla_I^2(\mathbf{R}) \rangle}{2m_I}, \tag{4.1}$$

where the averaging of the adiabatic correction term is performed using the electronic wave function. The latter term is mass-dependent.

A highly accurate local fit of $E_{\mathrm{tot}}(\mathbf{R})$ has been obtained for the D_3^+ isotopologue in a polynomial form. In contrast to the previous work, the total energy has been fitted directly, rather than through separate fits for each term in equation (4.1). The analytical form of the fit is

$$V(\mathbf{R}) = P^N(\Gamma_1, \Gamma_2, \Gamma_3) = \sum_{i+2j+3k \le N} c_{ijk} \Gamma_1^i \Gamma_2^j \Gamma_3^k, \tag{4.2}$$

where the basis functions, Γ_i, are defined in terms of symmetry coordinates, Q_i, as

$$\Gamma_1 = Q_1, \quad \Gamma_2 = Q_2^2 + Q_3^2 \quad \text{and} \quad \Gamma_3 = Q_3(Q_3^2 - 3Q_2^2). \tag{4.3}$$

These functions form the so-called integrity basis [67] and thus any product of them is totally symmetric with respect to any permutation of the three nuclei. The symmetry coordinates have the following well-known form:

$$\begin{pmatrix} Q_1 \\ Q_2 \\ Q_3 \end{pmatrix} = \begin{pmatrix} \sqrt{\frac{1}{3}} & \sqrt{\frac{1}{3}} & \sqrt{\frac{1}{3}} \\ 0 & \sqrt{\frac{1}{2}} & -\sqrt{\frac{1}{2}} \\ \sqrt{\frac{2}{3}} & -\sqrt{\frac{1}{6}} & \sqrt{\frac{1}{6}} \end{pmatrix} \begin{pmatrix} \tilde{R}_1 \\ \tilde{R}_2 \\ \tilde{R}_3 \end{pmatrix}, \tag{4.4}$$

in terms of the expansion coordinates, $\tilde{R}_i$, for which we use, following Meyer *et al.* [68], the Morse displacement coordinates

$$\tilde{R}_i = \frac{1 - \mathrm{e}^{-\beta_\alpha (R_i/R_{0,\alpha} - 1)}}{\beta_\alpha}. \tag{4.5}$$

Table 2. Lowest band origins of D_3^+, derived from experiment (exp) and computed using nuclear masses (nuc) and effective masses (AIM).

(v_1, v_2^ℓ)	exp	nuc	exp − nuc	AIM	exp − AIM
$(0, 1^1)$	1834.674	1834.733	−0.059	1834.639	0.035
$(1, 0^0)$	2300.843	2301.198	−0.355	2301.076	−0.233
$(0, 2^0)$	3530.385	3530.650	−0.265	3530.477	−0.092
$(0, 2^2)$	3650.658	3650.829	−0.171	3650.644	0.014
$(1, 1^1)$	4059.470	4060.090	−0.620	4059.881	−0.411
$(2, 0^0)$	4553.792	4554.771	−0.979	4554.530	−0.738

Our fit for D_3^+ covers the energy region up to 30 000 cm^{-1} above the minimum. Some 4249 data points on our dense grid fall into this energy region. In obtaining the fit, a polynomial of degree $N = 16$ with 204 coefficients has been used. The root-mean-square deviation for the fit (of $\approx 4.5 \times 10^{-3}$ cm^{-1}) is one order of magnitude better than for our global fit GLH3P [6] obtained for the same energy region. For up to 20 000 cm^{-1}, the maximum deviation is only about 0.01 cm^{-1}.

In 1994, Amano *et al.* [69] analysed the available spectroscopic data of D_3^+ and fitted the rovibrational transition frequencies (529 lines) to a six-parameter model Hamiltonian. The transitions correspond to the following vibrational bands: $(0,0^0)$–$(0,1^1)$, $(0,0^0)$–$(0,2^2)$, $(0,1^1)$–$(0,2^0)$, $(0,1^1)$–$(0,2^2)$, $(0,2^0)$–$(0,3^3)$, $(0,2^2)$–$(0,3^1)$, $(1,0^0)$–$(1,1^1)$ and $(1,1^1)$–$(1,2^2)$, observed in the absorption and emission spectra. No further spectroscopic measurements have been carried out since then. The band origins derived by Amano *et al.* [69] are shown in table 2 and are compared there with our theoretical predictions. We note the relatively large differences for the $(1,0^0)$, $(1,1^1)$ and $(2,0^0)$ bands, where the latter band origin is derived from the model Hamiltonian and not directly supported by experimental data. However, if one directly compares each observed transition frequency with the corresponding computed one, one finds that most of the transitions are reproduced within about 0.045 cm^{-1}. This root-mean-square value was obtained in an analysis of all rovibrational transitions with $J \leq 10$, a total of 381 lines, which are compared in the electronic supplementary material, tables S3–S10. The deviations do not scale with J, which indicates that the use of the nuclear rotational reduced mass is adequate. It seems that the experimentally derived band origins are perhaps not accurate for some states. A similar observation has been made by Polyansky & Tennyson [30] and shows that H_3^+ and isotopologues are difficult to describe with model Hamiltonians. MARVEL energy levels should not suffer from this problem; however, the number of measured D_3^+ lines is not sufficient for such an analysis [66].

5. Conclusion

Non-adiabatic coupling to excited electronic states causes energy shifts to the rovibrational energy values computed on the electronic ground state potential energy surface of up to 2 cm^{-1}. Strategies to include non-adiabatic effects in the rovibrational computations are presented. The so far most successful approaches consist in using coordinate-dependent reduced masses for vibration and rotation. These can be constructed empirically. The iterative stockholder atoms-in-molecules approach provides a general access to the vibrational reduced mass. Its application, together with the use of a very accurate potential energy surface comprising the Born–Oppenheimer energy, diagonal adiabatic correction terms as well as relativistic and QED correction terms, has led to the most accurate energy levels obtained so far for H_3^+ and D_3^+, which approach the experimentally determined values to within a fraction of a wavenumber.

Data accessibility. Electronic supplementary material is available online at rs.figshare.com.

Authors' contributions. P.H.R.A. developed and coded the AIM method to obtain reduced masses, and computed and processed the D_3^+ data. M.S. computed the QED corrections. L.A. developed the QED and electronic

structure codes. L.G.D. developed the Mulliken-based reduced masses. J.R.M. and A.A. are PhD supervisors of P.H.R.A. A.A. drafted the manuscript and analysed, with P.H.R.A., the D_3^+ data. All authors read and approved the manuscript.

Competing interests. We declare we have no competing interests.

Funding. A.A. acknowledges support given by the COST MOLIM project (CM1405) and by the Programme National de Planétologie (PNP) of CNRS/INSU, co-funded by CNES. This work was also partially supported by funds from the Polish National Science Centre granted on the basis of Decision no. DEC-2013/10/E/ST4/00033. Support from the Brazilian agencies CNPq and FAPEMIG is also acknowledged.

Acknowledgements. The authors thank the high-performance computer centres ROMEO of the University of Reims Champagne-Ardenne and CRIANN of the Region of Normandy for generous allowance of super-computer time.

References

1. Slater JC. 1928 Central fields and Rydberg formulas in wave mechanics. *Phys. Rev.* **31**, 333–343. (doi:10.1103/PhysRev.31.333)
2. Kato T. 1957 On the eigenfunctions of many-particle systems in quantum mechanics. *Commun. Pure Appl. Math.* **10**, 151–177. (doi:10.1002/cpa.3160100201)
3. Cencek W, Rychlewski J, Jaquet R, Kutzelnigg W. 1998 Sub-microhartree accuracy potential energy surface for H_3^+ including adiabatic and relativistic effects. I. Calculation of the potential points. *J. Chem. Phys.* **108**, 2831–2836. (doi:10.1063/1.475702)
4. Lodi L, Polyansky OL, Tennyson J, Alijah A, Zobov NF. 2014 QED correction for H_3^+. *Phys. Rev. A* **89**, 032505. (doi:10.1103/PhysRevA.89.032505)
5. Bachorz RA, Cencek W, Jaquet R, Komasa J. 2009 Rovibrational energy levels of H_3^+ with energies above the barrier to linearity. *J. Chem. Phys.* **131**, 024105. (doi:10.1063/1.3167795)
6. Pavanello M *et al.* 2012 Calibration-quality adiabatic potential energy surfaces for H_3^+ and its isotopologues. *J. Chem. Phys.* **136**, 184303. (doi:10.1063/1.4711756)
7. Mizus II, Polyansky OL, McKemmish LK, Tennyson J, Alijah A, Zobov NF. 2018 A global potential energy surface for H_3^+. *Mol. Phys.* **117**, 1663–1672. (doi:10.1080/00268976.2018.1554195)
8. Tennyson J, Polyansky OL, Zobov NF, Alijah A, Császár AG. 2017 High-accuracy calculations of the rotation–vibration spectrum of H_3^+. *J. Phys. B: At. Mol. Opt. Phys.* **50**, 232001. (doi:10.1088/1361-6455/aa8ca6)
9. Adamowicz L, Stanke M *et al.* In preparation.
10. Kołos W, Wolniewicz L. 1963 Nonadiabatic theory for diatomic molecules and its application to the hydrogen molecule. *Rev. Mod. Phys.* **35**, 473–483. (doi:10.1103/RevModPhys.35.473)
11. Pachucki K. 2013 Efficient approach to two-center exponential integrals with applications to excited states of molecular hydrogen. *Phys. Rev. A* **88**, 022507. (doi:10.1103/PhysRevA.88.022507)
12. Pachucki K, Komasa J. 2018 Nonadiabatic rotational states of the hydrogen molecule. *Phys. Chem. Chem. Phys.* **20**, 247–255. (doi:10.1039/C7CP06516G)
13. Czachorowski P, Puchalski M, Komasa J, Pachucki K. 2018 Nonadiabatic relativistic correction in H_2, D_2, and HD. *Phys. Rev. A* **98**, 052506. (doi:10.1103/PhysRevA.98.052506)
14. Puchalski M, Komasa J, Czachorowski P, Pachucki K. 2019 Nonadiabatic QED correction to the dissociation energy of the hydrogen molecule. *Phys. Rev. Lett.* **122**, 103003. (doi:10.1103/physrevlett.122.103003)
15. Nakashima H, Nakatsuji H. 2018 Solving the Schrödinger equation of hydrogen molecule with the free complement–local Schrödinger equation method: potential energy curves of the ground and singly excited singlet and triplet states, Σ, Π, Δ, and Φ. *J. Chem. Phys.* **149**, 244116. (doi:10.1063/1.5060659)
16. Kurokawa YI, Nakashima H, Nakatsuji H. 2019 Solving the Schrödinger equation of hydrogen molecules with the free-complement variational theory: essentially exact potential curves and vibrational levels of the ground and excited states of the Σ symmetry. *Phys. Chem. Chem. Phys.* **21**, 6327–6340. (doi:10.1039/c8cp05949g)
17. Herman RM, Asgharian A. 1966 Theory of energy shifts associated with deviations from Born-Oppenheimer behavior in $^1\Sigma$-state diatomic molecules. *J. Mol. Spectrosc.* **19**, 305–324. (doi:10.1016/0022-2852(66)90254-2)

18. Bunker PR, Moss RE. 1977 The breakdown of the Born–Oppenheimer approximation: the effective vibration–rotation hamiltonian for a diatomic molecule. *Mol. Phys.* **33**, 417–424. (doi:10.1080/00268977700100351)
19. Kutzelnigg W. 2007 Which masses are vibrating or rotating in a molecule? *Mol. Phys.* **105**, 2627–2647. (doi:10.1080/00268970701604671)
20. Jaquet R, Kutzelnigg W. 2008 Non-adiabatic theory in terms of a single potential energy surface. The vibration–rotation levels of H_2^+ and D_2^+. *Chem. Phys.* **346**, 69–76. (doi:10.1016/j.chemphys.2008.02.068)
21. Mátyus E. 2018 Non-adiabatic mass correction to the rovibrational states of molecules: numerical application for the H_2^+ molecular ion. *J. Chem. Phys.* **149**, 194111. (doi:10.1063/1.5050401)
22. Mátyus E. 2018 Non-adiabatic mass-correction functions and rovibrational states of $^4He_2^+$ ($X\,^2\Sigma_u^+$). *J. Chem. Phys.* **149**, 194112. (doi:10.1063/1.5050403)
23. Bunker PR, Moss RE. 1980 Effect of the breakdown of the Born–Oppenheimer approximation on the rotation–vibration Hamiltonian of a triatomic molecule. *J. Mol. Spectrosc.* **80**, 217–228. (doi:10.1016/0022-2852(80)90283-0)
24. Schwenke DW. 2001 Beyond the potential energy surface: *ab initio* corrections to the Born–Oppenheimer approximation for H_2O. *J. Phys. Chem. A* **105**, 2352–2360. (doi:10.1021/jp0032513)
25. Khoma M, Jaquet R. 2017 The kinetic energy operator for distance-dependent effective nuclear masses: derivation for a triatomic molecule. *J. Chem. Phys.* **147**, 114106. (doi:10.1063/1.5000267)
26. Jaquet R, Khoma MV. 2017 Investigation of nonadiabatic effects for the vibrational spectrum of a triatomic molecule: the use of a single potential energy surface with distance-dependent masses for H_3^+. *J. Phys. Chem. A* **121**, 7016–7030. (doi:10.1021/acs.jpca.7b04703)
27. Jaquet R, Khoma MV. 2018 Investigation of non-adiabatic effects for the ro-vibrational spectrum of H_3^+: the use of a single potential energy surface with geometry-dependent nuclear masses. *Mol. Phys.* **116**, 3507–3518. (doi:10.1080/00268976.2018.1464225)
28. Holka F, Szalay PG, Fremont J, Rey M, Peterson KA, Tyuterev VG. 2011 Accurate *ab initio* determination of the adiabatic potential energy function and the Born–Oppenheimer breakdown corrections for the electronic ground state of LiH isotopologues. *J. Chem. Phys.* **134**, 094306. (doi:10.1063/1.3555758)
29. Moss RE. 1996 On the adiabatic and nonadiabatic corrections in the ground electronic state of the hydrogen molecular cation. *Mol. Phys.* **89**, 195. (doi:10.1080/002689796174083)
30. Polyansky OL, Tennyson J. 1999 *Ab initio* calculation of the rotation–vibration energy levels of H_3^+ and its isotopomers to spectroscopic accuracy. *J. Chem. Phys.* **110**, 5056–5064. (doi:10.1063/1.478404)
31. Alijah A, Hinze J. 2006 Rotation–vibrational states of H_3^+ and the adiabatic approximation. *Phil. Trans. R. Soc. A* **364**, 2877–2888. (doi:10.1098/rsta.2006.1860)
32. Alijah A, Andrae D, Hinze J. 2010 An empirical formula to estimate off-diagonal adiabatic corrections to rotation–vibrational energy levels. *Theor. Chem. Acc.* **127**, 149–155. (doi:10.1007/s00214-009-0710-1)
33. Alijah A, Hinze J, Wolniewicz L. 1995 Rotation–vibrational states of H_2D^+ using hyperspherical coordinates and harmonics. *Mol. Phys.* **85**, 1105–1123. (doi:10.1080/00268979500101701)
34. Alijah A, Beuger M. 1996 Rotation–vibrational states of D_2H^+ computed using hyperspherical harmonics. *Mol. Phys.* **88**, 497–516. (doi:10.1080/00268979650026497)
35. Alijah A, Wolniewicz L, Hinze J. 1995 Rotation–vibrational states of D_3^+ computed using hyperspherical harmonics. *Mol. Phys.* **85**, 1125–1150. (doi:10.1080/00268979500101711)
36. Schiffels P, Alijah A, Hinze J. 2003 Rovibrational states of H_3^+. Part 1: The energy region below 9000 cm^{-1} and modelling of the non-adiabatic effects. *Mol. Phys.* **101**, 175. (doi:10.1080/00268970210158687)
37. Watson JKG. 1984 Higher-order vibration–rotation energies of the X_3 molecule. *J. Mol. Spectrosc.* **103**, 350–363. (doi:10.1016/0022-2852(84)90062-6)
38. Schiffels P, Alijah A, Hinze J. 2003 Rovibrational states of H_3^+. Part 2: The energy region between 9000 cm^{-1} and 13 000 cm^{-1} including empirical corrections for the non-adiabatic effects. *Mol. Phys.* **101**, 189. (doi:10.1080/00268970210158713)

39. Alijah A. 2010 Accurate calculations and assignments of above-barrier states of H_3^+ up to 15 300 cm^{-1}. *J. Mol. Spectrosc.* **264**, 111–119. (doi:10.1016/j.jms.2010.09.009)
40. Kreckel H, Bing D, Reinhardt S, Petrignani A, Berg M, Wolf A. 2008 Chemical probing spectroscopy of H_3^+ above the barrier to linearity. *J. Chem. Phys.* **129**, 164312. (doi:10.1063/1.2994730)
41. Morong CP, Gottfried JL, Oka T. 2009 H_3^+ as the benchmark for rigorous *ab initio* theory. *J. Mol. Spectrosc.* **255**, 13–23. (doi:10.1016/j.jms.2009.02.010)
42. Berg M, Wolf A, Petrignani A. 2012 Visible transitions from ground state H_3^+ measured with high-sensitivity action spectroscopy. *Phil. Trans. R. Soc. A* **370**, 5028–5040. (doi:10.1098/rsta.2012.0017)
43. Neale L, Miller S, Tennyson J. 1995 Spectroscopic properties of the H_3^+ molecule: a new calculated line list. *Astrophys. J.* **464**, 516–520. (doi:10.1086/177341)
44. Pavanello M *et al.* 2012 Precision measurements and computations of transition energies in rotationally cold triatomic hydrogen ions up to the midvisible spectral range. *Phys. Rev. Lett.* **108**, 023002. (doi:10.1103/PhysRevLett.108.023002)
45. Mohallem JR, Diniz LG, Dutra AS. 2011 Separation of motions of atomic cores and valence electrons in molecules. *Chem. Phys. Lett.* **501**, 575–579. (doi:10.1016/j.cplett.2010.11.047)
46. Diniz LG, Alijah A, Mohallem JR. 2012 Core-mass nonadiabatic corrections to molecules: H_2, H_2^+, and isotopologues. *J. Chem. Phys.* **137**, 164316. (doi:10.1063/1.4762442)
47. Wolniewicz L, Poll JD. 1986 On the higher vibration rotational levels of HD^+ and H_2^+. *Mol. Phys.* **59**, 953–964. (doi:10.1080/00268978600102501)
48. Wolniewicz L. 1993 Relativistic energies of the ground-state of the hydrogen molecule. *J. Chem. Phys.* **99**, 1851–1868. (doi:10.1063/1.465303)
49. Wolniewicz L. 1995 Nonadiabatic energies of the ground-state of the hydrogen molecule. *J. Chem. Phys.* **103**, 1792–1799. (doi:10.1063/1.469753)
50. Diniz LG, Mohallem JR, Alijah A, Pavanello M, Adamowicz L, Polyansky O, Tennyson J. 2013 Rotational and vibrational non-adiabatic calculations on H_3^+ using coordinate-dependent vibrational and rotational masses. *Phys. Rev. A* **88**, 032506. (doi:10.1103/PhysRevA.88.032506)
51. Alijah A, Duxbury G. 1990 Renner-Teller and spin-orbit interactions between the $^1A_1$, $^1B_1$ and $^3B_1$ states of CH_2. *Mol. Phys.* **70**, 605–622. (doi:10.1080/00268979000102621)
52. Mátyus E, Szidarovszky T, Császár AG. 2014 Modelling non-adiabatic effects in H_3^+: solution of the rovibrational Schrödinger equation with motion-dependent masses and mass surfaces. *J. Chem. Phys.* **141**, 154111. (doi:10.1063/1.4897566)
53. Tennyson J, Henderson JR, Fulton NG. 1995 DVR3D. *Comput. Phys. Commun.* **86**, 175. (doi:10.1016/0010-4655(94)00139-S)
54. Wu KY, Lien YH, Liao CC, Lin YR, Shy JT. 2013 Measurement of the ν_2 fundamental band of H_3^+. *Phys. Rev. A* **88**, 032507. (doi:10.1103/PhysRevA.88.032507)
55. Mátyus E, Czakó G, Császár AG. 2009 Toward black-box-type full- and reduced-dimensional variational (ro)vibrational computations. *J. Chem. Phys.* **130**, 134112. (doi:10.1063/1.3076742)
56. Mulliken RS. 1936 The low electronic states of simple heteropolar diatomic molecules. II. Alkali metal hydrides. *Phys. Rev.* **50**, 1028–1040. (doi:10.1103/PhysRev.50.1028)
57. Coxon JA, Dickinson CS. 2004 Application of direct potential fitting to line position data for the $X^1\Sigma^+$ and $A^1\Sigma^+$ states of LiH. *J. Chem. Phys.* **121**, 9378–9388. (doi:10.1063/1.1788659)
58. Diniz LG, Alijah A, Adamowicz L, Mohallem JR. 2015 Connecting a new non-adiabatic vibrational mass to the bonding mechanism of LiH: a quantum superposition of ionic and covalent states. *Chem. Phys. Lett.* **633**, 89–94. (doi:10.1016/j.cplett.2015.04.062)
59. Diniz LG, Kirnosov N, Alijah A, Mohallem JR, Adamowicz L. 2016 Accurate dipole moment curve and non-adiabatic effects on the high resolution spectroscopic properties of the LiH molecule. *J. Mol. Spectrosc.* **322**, 22–28. (doi:10.1016/j.jms.2016.03.001)
60. Diniz LG, Alijah A, Mohallem JR. 2018 Benchmark linelists and radiative cooling functions for LiH isotopologues. *Astrophys. J. Suppl. Ser.* **235**, 35. (doi:10.3847/1538-4365/aab431)
61. Amaral PHR, Mohallem JR. 2017 Core–valence stockholder AIM analysis and its connection to nonadiabatic effects in small molecules. *J. Chem. Phys.* **146**, 194103. (doi:10.1063/1.4983394)
62. Hirshfeld FL. 1977 Bonded-atom fragments for describing molecular charge densities. *Theor. Chim. Acta* **44**, 129–138. (doi:10.1007/BF00549096)

63. Bultinck P, Cooper DL, Van-Neck D. 2009 Comparison of the Hirshfeld-I and iterated stockholder atoms in molecules schemes. *Phys. Chem. Chem. Phys.* **11**, 3424–3429. (doi:10.1039/b821734c)
64. Jaquet R, Khoma MV. 2012 Nonadiabatic investigations of ro-vibrational frequencies within the systems H_2^+, H_2, and prospects for H_3^+: use of distance-dependent effective masses. *Mol. Phys.* **110**, 669–683. (doi:10.1080/00268976.2012.671969)
65. Jaquet R, Carrington T. 2013 Using a nondirect product basis to compute $J > 0$ rovibrational states of H_3^+. *J. Phys. Chem. A* **117**, 9493–9500. (doi:10.1021/jp312027s)
66. Furtenbacher T, Szidarovszky T, Mátyus E, Fábri C, Császár AG. 2013 Analysis of the rotational-vibrational states of the molecular ion H_3^+. *J. Chem. Theory Comput.* **9**, 5471–5478. (doi:10.1021/ct4004355)
67. Weyl H. 1946 *The classical theory of groups*. Princeton, NJ: Princeton University Press.
68. Meyer W, Botschwina P, Burton PR. 1986 *Ab initio* calculation of near-equilibrium potential and multipole moment surfaces and vibrational frequencies of H_3^+ and its isotopomers. *J. Chem. Phys.* **84**, 891–900. (doi:10.1063/1.450534)
69. Amano T, Chan MC, Civiš S, McKellar ARW, Majewski WA, Sadovskií D, Watson JKG. 1994 The infrared vibration–rotation spectrum of the D_3^+ molecular ion: extension to higher vibrational and rotational quantum numbers. *Can. J. Phys.* **72**, 1007–1015. (doi:10.1139/p94-132)